Numerical Methods in Civil Engineering, 5-3 (2021) 34-45

Numerical Methods in Civil Engineering

Journal Homepage: https://nmce.kntu.ac.ir/

Evaluation of site effects on the seismic performance of a friction-damped steel IMF under near-fault earthquakes

Arsam Taslimi*, Shayan Safaei**

ARTICLE INFO

RESEARCH PAPER

Article history:
Received:
January 2021.
Revised:
February 2021.
Accepted:
March 2021.

Keywords:
Site Effects,
Friction Damper,
Steel Moment Frame,
Hysteresis Curves,
Near-Fault Earthquakes

Abstract:

The local site conditions and the geological properties of soil materials on which buildings are constructed might play a pivotal role in changing the characteristics of input seismic ground motions, and subsequently affect the seismic performance of the structures. These effects should be considered in the seismic evaluation of structures, especially those equipped with damping devices. As a matter of fact, these devices are designed to increase the energy dissipation capacity of the buildings through certain inelastic mechanisms, which are highly dependent on the input ground motions. Friction dampers are one of the cost-efficient controlling devices in which whose performance mostly depends on the story displacements. Hence, the variation in seismic excitations caused by the local site effects might have an impact on how they mitigate the earthquake hazard in addition to their efficiency. Shedding light on the above facts, this paper evaluates the influence of site effects on the seismic performance of a 10-story intermediate friction-damped steel moment frame under near-field excitations. Nonlinear time-history analyses are done using ten ground motions, which have been originally recorded at bedrock, while variation in their properties is calculated by passing them through a soil profile, which is modelled using the equivalent linear method. The result indicates that considering the site soil effects has a major consequence on ground motions as well as the performance of dampers insofar as it leads to a rise in the amount of input energy and the story drifts. Nevertheless, the seismic performance of the dampers remain quite efficient and reliable.

1. Introduction

Innovative cost-efficient solutions to mitigate the inelastic demand triggered by structural members of a frame building during strong earthquakes have been introduced by previous studies (Ramirez and Tirca, 2012; Voica & Stratan, 2020). Energy dissipation devices have been under development during the last decades, and there is a growing tendency in their implementation (Symans et al., 2008). These devices range from passive energy dissipation systems such as viscous fluid dampers (Lee & Taylor, 2001), viscoelastic solid dampers (Bergman & Hanson, 1993), metallic hysteretic dampers (Whittaker et al., 1991), and friction dampers (Pall, 1979) to active and semi-active systems. Meanwhile, due to their high cost-efficiency, friction dampers have been popular both in the research and engineering communities.

* *Corresponding Author: Ph.D. Candidate, Department of Civil & Environmental Engineering, University of Nevada, Reno, United States, Email: rsamtaslimi@nevada.unr.edu*
** *Master of Science, Amirkabir University of Technology, Tehran, Iran*

Pioneering work on friction dampers was firstly reported by Pall (1979). These dampers are well-known for their low-cost and maintenance-free characteristics resulting in a wide range of applications for new construction as well as retrofit of existing buildings (Pall and Pall, 2004). The aforementioned devices rely on the resistance developed between two solid interfaces sliding relative to one another. During severe seismic excitations, the device slips at a predetermined load, providing the desired energy dissipation by friction whilst at the same time shifting the structural fundamental mode away from the earthquake resonant frequency (Vaseghi et al., 2009). Pall (1979) had also reported that the most stable behavior under static and dynamic loading was obtained when brake lining pads in contact with mill scale surface on the plate were chosen. These kinds of dampers have successfully undergone rigorous proof testing in the U.S and Canada. In 1985, the National Research Council of Canada tested a 3-story frame structure on a shaking table at the University of British Columbia, Vancouver (Filiatrault and Cherry, 1986).

Besides, in 1986-1987, the U.S. National Science Foundation tested a 9-story frame structure on a shaking table at the University of California at Berkeley (Aiken et al., 1988). The structures were subjected to more than 20 different strong ground motion records. Even for an earthquake five times stronger than the 1985-Mexico earthquake, the frames equipped with friction dampers remained damage free (Pall and Pall, 2004).

There are cogent arguments in the literature indicating that the geological features of soil materials beneath a site have a striking impact on seismic properties of earthquake waves (Sanchez-Sesma, 1987; Aki, 1993; Wen et al., 2006; Panah & Nouri, 2016; Ali & Ali, 2020). This phenomenon, known as the local site effect, was first highlighted by Anderson et al. (1986) for the 1985 Michoacan earthquake in Mexico. The repercussions of local site effects during extreme earthquakes have also drawn researchers' attention (Trifunac, 2016). For instance, the building losses associated with the local site effects of Izmit 1999 (Bakir et al., 2002), L'Aquila 2009 (Cultrera et al., 2011), Lorca 2011 (Navarro et al., 2012) earthquakes have been studied, and the important role of site conditions in the damage distribution has been unveiled. Seismic site effects in Tehran, Iran, are evaluated by Behrou et al. (2017), where they compared the estimated site response spectra with the suggested response spectra in the Iranian code (BHRC, 2014). They indicated that there is a significant disparity between the estimated response spectra and the one in the Iranian code. The results also showed a substantial contribution of site effects on ground motion response in majority parts of the studied area (Behrou et al., 2018).

Since the friction dampers have been employed broadly as a practical solution to reduce the detrimental impacts of earthquakes on both steel (Sadeghi et al., 2020) and RC structures (Nabid et al., 2020), a growing body of literature has been attributed to different aspects of their application and behavior (Mazza et al., 2013, Khansefid & Ahmadizadeh, 2016, Tirca, 2015). The seismic fragility of friction damped braced frames under the action of strong earthquakes is evaluated to find the optimal range of the slip force of the device and the stiffness ratio of the system (Taiyari et al., 2019). Moreover, the need for developing fragility models that account for soil-structure interaction and specific structural and ground conditions, data gathered from Mexico-Puebla 2017 earthquake has also been studied (Román-De La Sancha et al., 2019) to ensure a more reliable risk characterization. The efficient placement of friction dampers on building structures with and without the effects of soil-structure interaction has also been executed (Sanghai & Pawade, 2019, Sanghai & Pawade, 2021, Bagchi et al., 2021). Nonetheless, the consequences that the local site effects might have on the performance of friction dampers have been overlooked.

In this paper, the effect of site soil on the seismic performance of a 10-story intermediate steel damped moment frame is evaluated under near-fault ground motions. To this end, first, a suite of ten ground motions, including pulse-like and non-pulse excitations which are initially recorded at the bedrock, are chosen. Then, the soil effects of a construction site located in Tehran, Iran, which is modelled in the platform of Deepsoil using the equivalent linear method, have been assessed on the ground motions. Finally, a series of nonlinear time-history analyses are performed to examine the seismic performance of the structure and the dampers with and without the consideration of the site effects. The results of this study show that despite the growing PGAs and input energies of the ground motions, the performance of the dampers are satisfactory. Further, the steel frames generally remain elastic as the majority of the input energy in all cases is absorbed by the dampers.

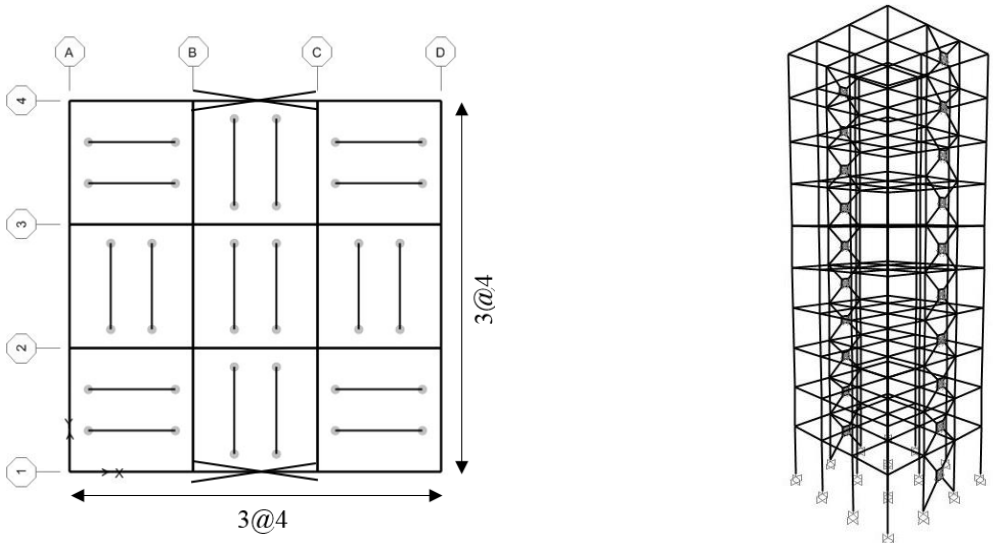

(a) (b)

Fig. 1: (a) The typical plan of the floors; (b) The 3D geometry of the structure (units in meter).

2. Preliminary Structure

The preliminary structure is a 10-story steel intermediate moment frame (IMF) building with three spans of 4-meter length in orthogonal directions. The total height of this building is 37.42-m in which the height of the first floor is 4.57, and the rest are 3.65 meters. The plan and the 3D view of the structure are shown in Fig. 1(a) and (b), respectively. This building is supposed to be located in Tehran, Iran, where the soil class is C, and the seismic hazard category is very high according to the Iranian seismic code, the so-called Standard No. 2800, (BHRC, 2014). The structure is modeled and designed in SAP2000 V.20.2.0 based on Standard No. 2800 provisions and in compliance with AISC 360-10 (AISC, 2010). The structure is an intermediate moment frame with metal deck slab floors, which is intentionally designed in a way that the stress ratio is appropriately controlled while the drift ratio is more than the allowable limits in some stories (see Table 2). Therefore, friction dampers are necessary to resolve this issue. The final designed sections are reported in Table 1.

Table 1: Designed sections of the preliminary structure

Story	Column	Story	Beam	Story	Secondary Beam
1-3	Box 300x300x25	1-3	IPE360o	1-9	IPE180
4-6	Box 300x300x20	4-6	IPE360		
7	Box 250x250x10	7-8	IPE330		
8-9	Box 200x200x15	9	IPE270		
10	Box 150x150x10	10	IPE220	10	IPE140

3. Design of the Friction Dampers

The method that has been used in this paper to design friction dampers was firstly presented by Filiatrault and Cherry (1990). This method is based on the concept of optimum slip-load distribution. For modeling friction dampers, the Plastic Wen links, as shown in Fig. 2, are employed. The key parameters of this model are the initial stiffness, post-yield stiffness, yield force, and yield exponent. Since the hysteresis loops are nearly rectangular in friction dampers, the initial stiffness is infinite, and the post-yield stiffness ratio is taken to be zero (Rigid-Perfectly Plastic response). The yield force is calculated by equally distributing the slip shear force of each floor between all of the friction dampers installed in that floor, and the yield exponent is assumed to be between 1 and 10 (Sepehri, 2016). As the height of the building on the first floor differs from the other stories, the characteristics of the dampers used in the first story are different. The yield force of 230 and 205kN is calculated for the dampers located in the 1st and the rest of the stories, respectively, while the yield exponent of 10 is considered for all of the dampers.

After designing the friction-damped structure under the design gravity and lateral loads, the story drifts are obtained. As represented in Table 2, the drift ratios that had not been controlled in the preliminary structure are under the allowable limits after inserting the dampers, indicating that the performance of dampers are satisfactory. It is worth mentioning that the allowable drift limit based on Standard No. 2800 is 0.02h.

Table 2: Drift ratios of the preliminary and friction-damped structures

Story	Preliminary Structure		Friction-damped Structure	
	Displacement (cm)	Drift	Displacement (cm)	Drift
10	26.30	0.030	10.98	0.014
9	23.52	0.029	9.68	0.014
8	20.91	0.035	8.37	0.015
7	17.69	0.029	7.04	0.014
6	15.05	0.027	5.75	0.013
5	12.59	0.029	4.53	0.013
4	9.94	0.030	3.35	0.012
3	7.24	0.028	2.28	0.010
2	4.72	0.027	1.36	0.008
1	2.24	0.020	0.60	0.005

4. Site Soil Characteristics

The characteristics of the site soil including maximum shear modulus, total unit weight, vertical effective stress and shear wave velocity as well as the soil profile, are obtained through in-situ tests, together with SPT (Standard Penetration test) and excavated boreholes for a construction site located in Tehran, Iran as reported in Table 3. Based on the test results, the numerical model of the soil profile is modelled in Deepsoil V.5.1 using the equivalent linear method. This profile is used to evaluate the changes in the earthquake ground motion characteristics, which are originally recorded at the bedrock, as they pass through the soil.

5. Ground Motions Characteristics

As mentioned earlier, the earthquake ground motions are recorded on the rock sites in which the shear wave velocity is higher than 760 m/s. The selected ground motions fall into two main categories: pulse-like and non-pulse records, each containing five ground motions recorded at the close distance of their faults (less than 15 Km according to ASCE7-16), and therefore classified as near-field records. They are so selected since the performance of friction

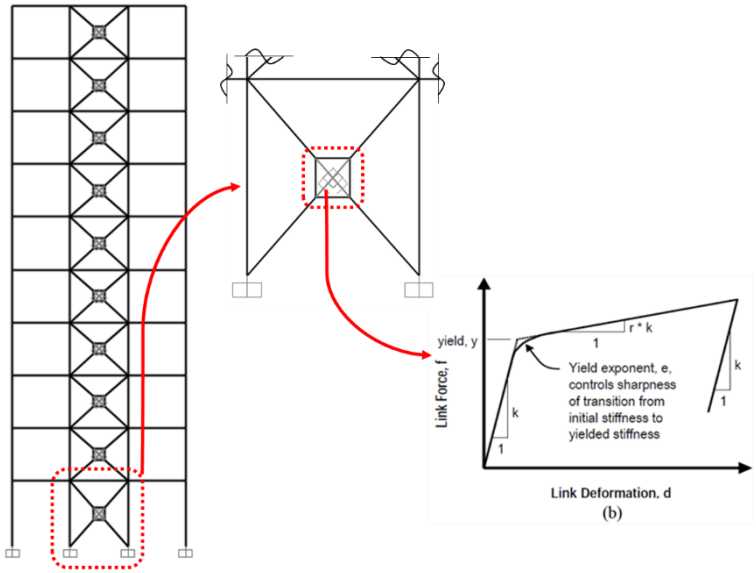

Fig. 2: Numerical modelling of friction dampers using Plastic Wen link

dampers which are highly dependent on the story displacement and drift, are more likely to be affected by near-field excitations, resulting in massive pulse-like lateral displacement in the buildings, especially those with intense pulses. The selected ground motions are obtained from NGA-West2 database (Ancheta et al., 2014). The characteristics of selected ground motions are summarized in Table 4, and the response spectra with 5% damping along with the design spectrum of standard No.2800 are given in Fig. 3.

6. Site Effect Evaluation on Ground Motions

The characteristics of the ground motions, including frequency content and peak ground acceleration (PGA) become exposed to change as the seismic waves pass through the different soil layers (Sanchez-Sesma, 1987; Aki, 1993; Kavand & Yazdi, 2019; Ali & Ali, 2020). These changes are assessed through modeling the soil layers of the site in Deepsoil and imposing the selected ground motions as input values. Generally speaking, there is no identical trend in the changes of the ground motions properties, yet there is a growth in the PGAs between 10 to 70% in most cases. The PGA values of each record at the top of each layer are presented in Fig. 4. In this figure, only the component with a higher PGA of each event is depicted. It should be noted that these variations are highly dependent on the soil properties and the ground motion itself.

Having used the equivalent linear method, the variation ratio, which is the variation of the PGA ratio of the ground motion at the top of the soil profile (at the site surface) to the ones recorded at the bedrock ($[PGA_{Surface}- PGA_{Bedrock}]/PGA_{Bedrock}$), is calculated and depicted in Fig. 5. Hereafter, for the sake of simplicity, the earthquake excitations recorded at the bedrock and those obtained from the top of the soil profile are called bedrock and surface ground motions, respectively.

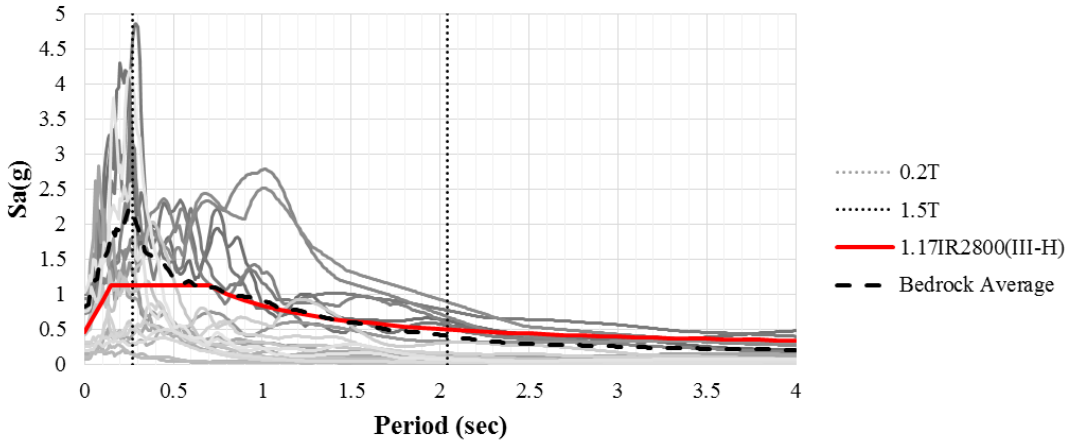

Fig. 3: 5 percent-damped response spectra of the selected ground motions

Table 3: The site soil layers properties

Layer	Soil Type	Thickness of layer (m)	Maximum Shear Modulus G_{max} (MPa)	Total Unit Weight (KN/m^3)	Vertical Effective Stress (KPa)	Shear Wave Velocity (m/s)
1	Clay	4.3	135.59	17.36	37.06	276.83
2	Sand	0.8	77.08	19.00	81.33	199.49
3	Sand	1.1	77.41	18.25	98.32	203.98
4	Clay	2.3	181.22	18.50	129.26	309.99
5	Clay	3.4	223.78	18.88	182.16	341.03
6	Sand	0.6	147.65	20.68	220.18	264.62
7	Sand	2.8	202.59	19.90	253.84	316.06
8	Sand	1.8	126.89	19.37	289.94	253.52
9(Bedrock)	-	-	1295.33	22.00	298.69	760

Table 4: A Summary of Ground Motions Characteristics

RSN	Event	Station	Year	Mechanism	M_w	V_s (m/s)	Type	T_p (s)
143	Tabas	Tabas	1978	Reverse	7.35	766.77	Pulse-like	6.18
1165	Kocaeli	Izmit	1999	Strike slip	7.51	811		5.36
3548	Loma Prieta	Los Gatos	1989	Reverse Oblique	6.93	1070.34		1.56
879	Landers	Lucerne	1992	Strike slip	7.28	1369		5.12
1161	Kocaeli	Gebze	1999	Strike slip	7.51	792		5.99
455	Morgan Hill	Gilroy Array #1	1984	Strike slip	6.19	1428.14	Non-pulse	-
765	Loma Prieta	Gilroy Array #1	1989	Reverse Oblique	6.93	1428.14		
1108	Kobe	Kobe University	1995	Strike slip	6.9	1043		
4083	Parkfield-02	Parkfield -Turkey Flat #1	2004	Strike slip	6	906.96		
8165	Duzce	IRIGM 496	1999	Strike slip	7.14	760		

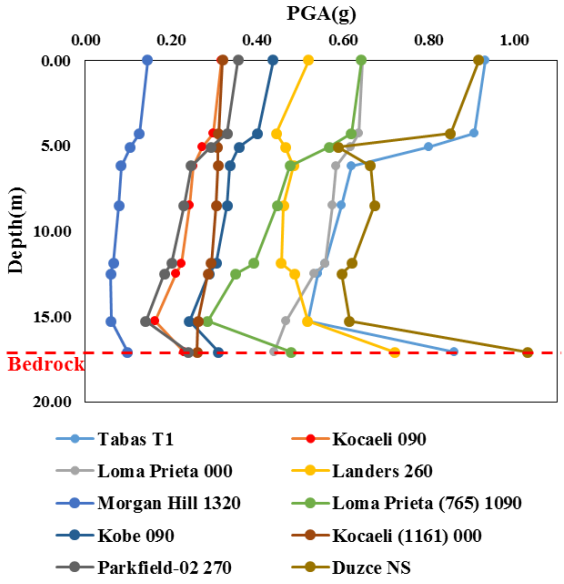

Fig. 4: PGA variation in different layers of the target soil profile

As can be seen in Fig. 5, the PGA of the records saw a rising trend from bedrock to the surface, except in five cases. The change in the records PGA varies widely, and in some cases, it is negative, which means the PGA of the surface is less than that of the bedrock. Showing the dispersion of the variation rate in the selected records, the PGA of the bedrock is plotted against the surface PGAs in Fig. 6, and a linear regression has been performed to calculate the coefficient of determination (the so-called R-square). Having an R-square of 0.8226 reveals the fact that the dispersion of the variation rate is nearly large, and the record-to-record changes do not follow the same path. Thus, the site effects differ depending on the properties of the soil layers and the input records. Additionally, the average variation rate for all of the ground motions is 24.58%, which means for the respective site of this study, the increase in the PGA of the records cannot be neglected. Therefore, ignorance of these effects might cause inaccurate responses when it comes to seismic performance assessment of structures.

Represented in Fig. 7 are the acceleration time-histories of Tabas and Duzce earthquakes, in which the pivotal role of the site effects on the frequency content and amplification of the ground accelerations is highlighted. Indeed, the soil layers act as a filter for seismic waves, and the ground motion characteristics would suffer from minor to major changes due to this effect. Besides, seismic waves may also be refracted or reflected as they pass from one layer to the other, and this can be the other source of these variations.

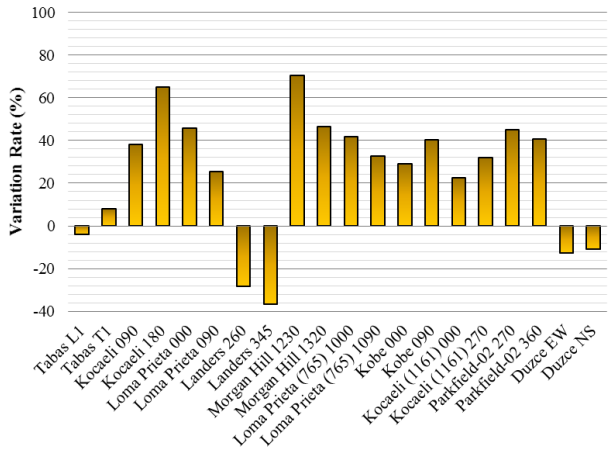

Fig. 5: The variation rate of the PGAs from bedrock to surface

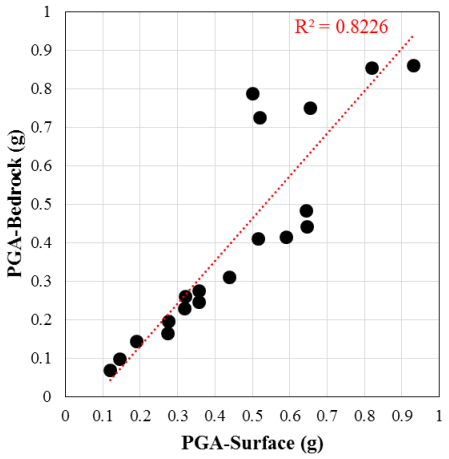

Fig. 6: Bedrock to surface PGA regression

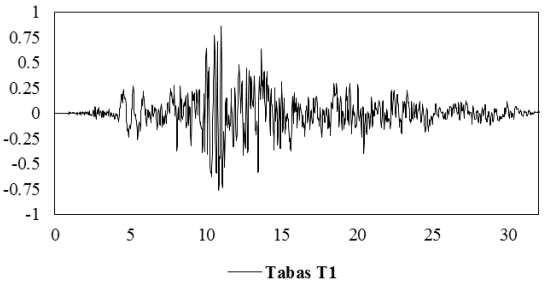

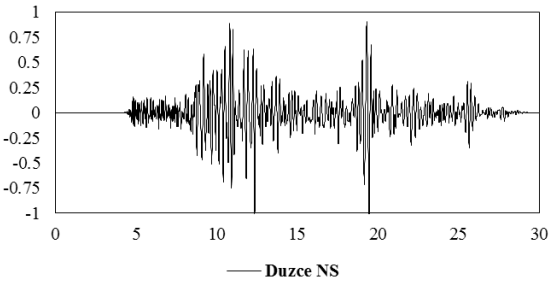

(a)

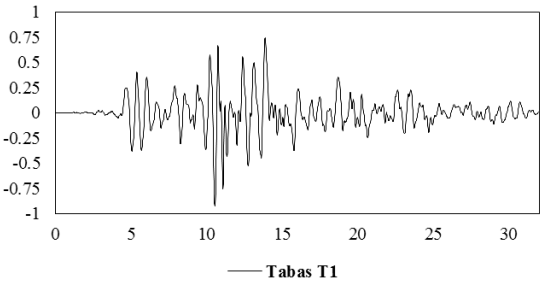

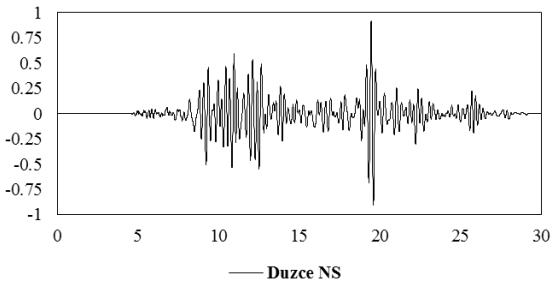

(b)

Fig. 7: Acceleration time-histories: (a) Bedrock records; (b) Surface records

7. Performance Assessment of Friction Dampers

Carrying out the nonlinear time-history analysis using the unprocessed (bedrock) and the processed (surface) ground motions, the seismic performance of friction dampers can be evaluated. The nonlinear time history analysis has been carried out using the Newmark-β (Newmark, 1959) method considering mass and stiffness proportional damping. It should be noted that these analyses have been done using the stronger component of each event. In other words, from each of the ten earthquake events presented in Table 4, only the horizontal component with larger PGA is applied to the building model in a direction that is controlled by the friction dampers. On the other hand, time-history analyses are done under two scenarios, including bedrock and surface records, to highlight the site effects on the building and dampers performance. Therefore, for each scenario, ten ground motions have been used for the analysis, the records of which were previously shown in Fig. 4. Based on the provisions of Standard No. 2800, all the ground motions need to be normalized and scaled. The scale factor is calculated through the method provided in Standard No. 2800. In this method, for each pair of horizontal ground motion components, a square root of the sum of the squares (SRSS) spectrum shall be calculated by taking the SRSS of the 5 percent-damped response spectra for the normalized components. The ground motion records should be scaled such that in the period range from 0.2T to 1.5T, the average of the SRSS spectra from all horizontal component pairs does not fall below 90% of the design spectrum of very high-risk zones for site class C.

Table 5: The ratio of input energy to the link hysteresis energy (%)

Pulse-like records				Non-pulse records		
Event	Bedrock	Surface		Event	Bedrock	Surface
Tabas-T1	76.12	63.58		MorganHill-1320	89.28	85.41
Kocaeli-090	63.03	61.58		Loma Prieta(765)-1090	76.23	70.11
Loma Prieta- 000	61.44	58.95		Kobe-090	67.60	67.20
Landers-260	74.63	61.18		Parkfield02-270	87.50	83.62
Kocaeli(1161)-000	74.10	69.41		Duzce-NS	87.40	82.27

Controlling the structures by increasing the systems' energy dissipation capacity is the main reason for using damping devices in structures. Therefore, as a measure for evaluating the efficacy of the friction dampers in the building model, the input energy produced by the input ground motions is compared to the amount of energy absorbed by all dampers. The ratio between the absorbed and input energy is calculated and given in Table 5. This ratio suffered a slight decline for all of the ten records, which means despite the fact that the frequency content and the ground motion characteristics have been changed due to the site effects, the dampers still work adequately and absorb the majority of the input energy to keep the structure in linear range and limit the damages to the frames. Presented in Fig. 8 are the graphs of the structure's input and absorbed energy variations with time excited by the unprocessed and the processed ground motions. As can be seen, the consideration of the local site effects caused a dramatic increase in the input energy, although the dampers could still absorb most of it.

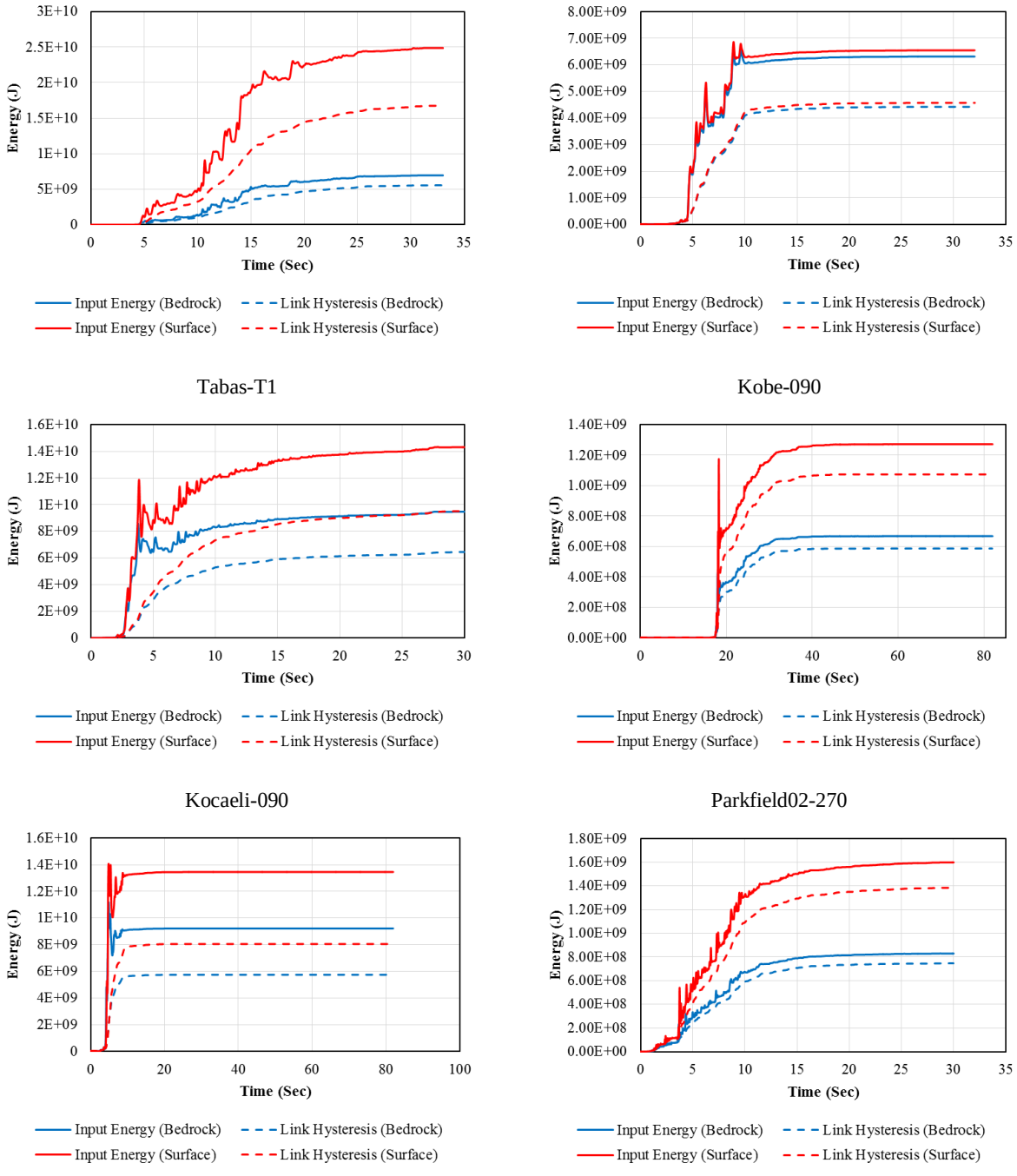

Fig. 8: The Input Energy and Link Hysteresis Energy of Friction Dampers: (a) Pulse-like records; (b) Non-pulse records

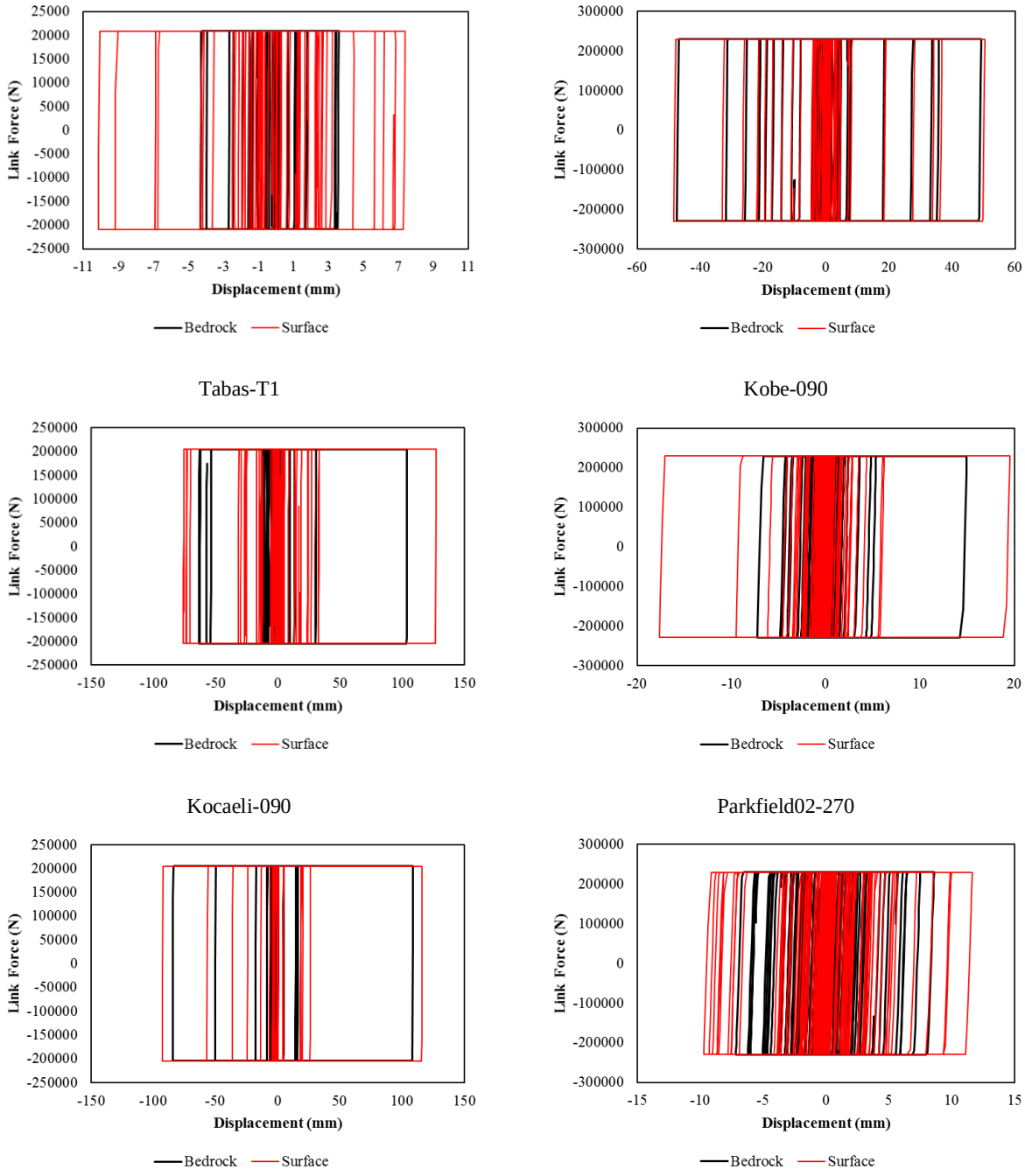

Fig. 9: Hysteresis Curves of Friction Dampers: (a) Pulse-like records; (b) Non-pulse records

To shed some light on the performance of each damper, a number of hysteretic curves are depicted in Fig. 9, in which for each record, the response curve of the damper located in the story with the greatest drift is chosen. For example, for Tabas-T1 and Loma Prieta-000, the maximum drift ratio occurred in story 7 and 6, respectively. As mentioned earlier, the hysteretic loops of friction dampers have a rectangular shape because of its large initial stiffness and nearly zero stiffness as it begins to displace. Looking at the curves under bedrock and surface ground motions, it can be realized that even for surface records, which usually cause more displacement, the dampers still have stable loops with high energy dissipation. For instance, although the displacements of the two ends of the dampers under Tabas-T1 and Prakfield02-270 records are nearly doubled for surface ground motions, the loops remain consistent, and the behavior of the dampers is acceptable.

It is worth noting that the changes in the amount of input energy and the stories' displacement saw no manifest pattern when pulse-like and non-pulse records are compared. For

instance, the input energy of Kobe-090, which is a non-pulse record, has slightly risen, whilst for Parkfield02-270, there is a dramatic increase in the input energy. Similar conclusions can also be derived from the hysteresis loops given in Fig. 9, which means that the adverse effects of the pulse-like records are not necessarily larger than that of the non-pulse records.

According to the above outcomes, it can be inferred that the local site effects on the input ground motions might well be significant, yet it varies from record to record and highly depends on the soil layers' characteristics. However, the performance of the friction dampers, which is profoundly related to the displacement of their ends, remains efficient and reliable as they dissipate most of the input energy through their unique mechanism. Thus, the structure equipped with these damping devices may be less sensitive to the site effect (variations in the characteristics of input ground motions) as they perform pretty well under the input motions.

8. Seismic Performance of the Building

Having conducted the time-history analyses using both sets of ground motions, the seismic performance of the building itself can also be investigated. As it was shown in Fig. 8, the input energy saw a dramatic rise when the surface records were imposed on the structure. This growing trend is summarized in Fig. 10 by comparing the base shear of the building when it is subjected to bedrock and surface records, respectively.

The maximum inter-story drift ratio (IDRMax) is one of the most important parameters when it comes to performance assessment of the structures. The initial IDRMax of the 10-story building structure used in this study exceeded the limits of the design code, but the insertion of the dampers improved its performance to the extent that the value of IDRMax was met in all the stories under the design lateral loads (refer to Table 2). However, it cannot be guaranteed that the building performance remains satisfactory under earthquake ground motions. Based on the characteristics of the input ground motions and the soil properties, the performance of the building can be affected differently. The graphs shown in Fig. 11 highlight the fact that despite the acceptable structural performance under the design loads, the IDRMax exceeds the code limit in some cases of bedrock records, but the average of inter-story drift ratios is still less than the allowable limit. However, the IDRMax has transgressed considerably as a result of the surface records, and the average IDRMax is slightly beyond the 2% limit in most stories. This indicates that the consideration of the site effects might have a striking influence on the global performance of the building, even if it was designed to mitigate the severe earthquake excitations. In other words, if the structural components of the building are not designed based on the surface ground motions, it is highly unlikely that the structure would meet all of the allowable seismic performance criteria. Given the maximum story acceleration presented in Fig. 12, which is another major parameter in the seismic performance evaluation, similar results can be concluded, and there is an increasing tendency in the story accelerations when the building is subjected to the surface records.

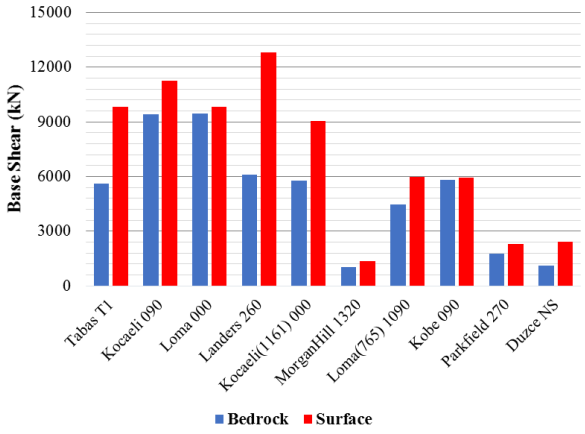

Fig. 10: The base shear of the building structure

In regards to the above observations, the site effects, which are mostly neglected in seismic performance assessment of the structures, have a strong potential to endanger the building performance, and turning a blind eye to these effects may lead to an unconservative design of the structures.

9. Conclusion

In this paper, the benefits of using friction dampers to improve the seismic performance of a steel moment frame, when the local site effects are considered, have been investigated. The structure is a 10-story steel IMF equipped with friction dampers located in Tehran, Iran, where the local site characteristics and the soil layers' properties are obtained from in-situ tests. The friction dampers are designed based on the method proposed by Filiatrault and Cherry (1990). A suite of ten near-field ground motions, including both pulse-like and non-pulse records all recorded initially at the bedrock, are chosen for time-history analysis. The numerical model of the site soil is developed in Deepsoil using the equivalent linear method. The recorded ground motions are applied to the soil profile to investigate their changes due to site effects. The derived ground motions from Deepsoil analysis are called surface records in which the frequency content and PGA are changed. Although there is no similar trend in the changes of the records, all of them

saw a variation in both PGA and frequency content due to the filtering effects of the soil layers.

Subsequently, the structure was subjected to the selected earthquakes under two scenarios, first using the original bedrock records and then using the surface records resulting from Deepsoil. The results of nonlinear time-history analyses indicated that the performance of these dampers remained acceptable in spite of the growing PGAs and input energies of the ground motions. Besides, most of the input energy in all cases absorbed by the dampers, such as elements of the friction-damped frames, are less likely to become nonlinear than the conventional steel frames, in which all the input energy needs to be dissipated by the beams or columns mechanisms. Hence the damages are mostly concentrated in the damping devices, and the frame elements are generally less contributed to dissipate the input energy. The hysteretic curves of the dampers are also stable and perfectly rectangular, even under the pulse-like surface records. Hence, the benefits accruing from the application of friction dampers in the building include a rise in structural safety and reliability as well as a reduction in sensitivity of the building to the local site effects. Correspondingly, the global seismic performance of the building indicates that the performance of the structure might be jeopardized by the local site effects if they are ignored during the evaluation and analysis, and these effects should be considered to ensure that a reliable and conservative design approach is achieved. However, the outcomes of this study are only limited to the specific site that is used as the input soil profile in Deepsoil. Therefore, the results of this research cannot necessarily be extended to other ground motions or sites.

Acknowledgment

This work represents the control of structures course project conducted at the Amirkabir University of Technology (AUT). The authors would like to express their appreciation and deep gratitude to the course lecturer, Prof. Taghikhany, for his valuable and constructive suggestions throughout this research.

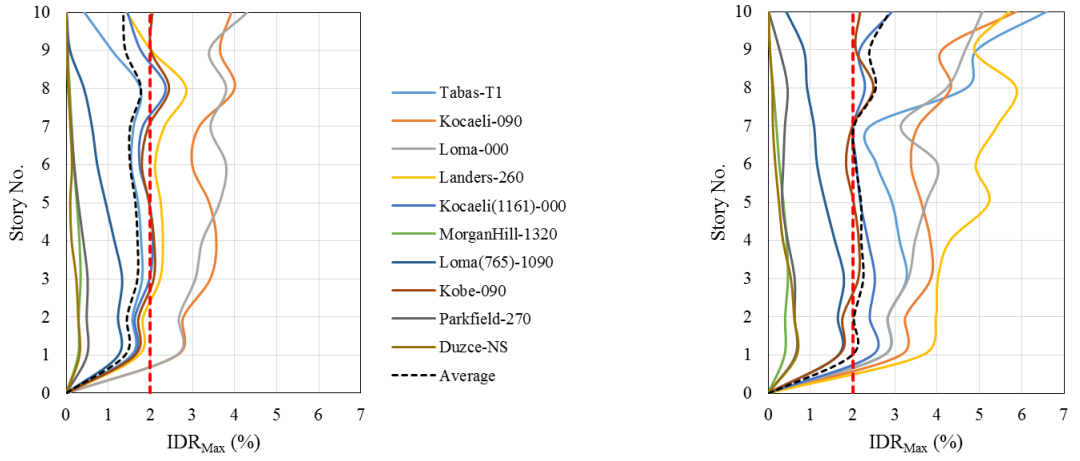

(a) (b)

Fig. 11: The maximum inter story drift ratio of the building under ground motions: (a) Bedrock (b) Surface

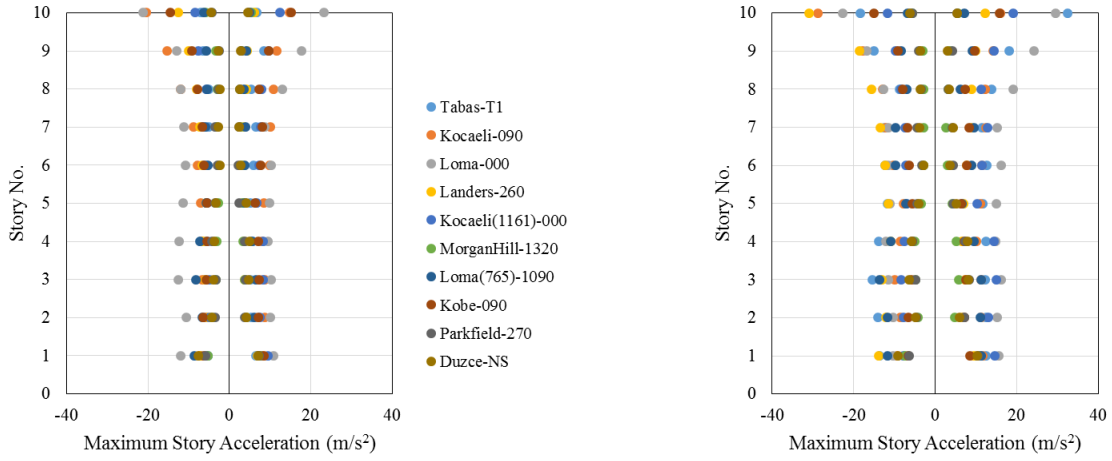

(a) (b)

Fig. 12: The maximum story acceleration of the building under ground motions: (a) Bedrock (b) Surface

References:

[1] Aiken, I. D., Kelly, J. M., & Pall, A. S. (1988). Seismic response of a nine-story steel frame with friction damped cross-bracing. Rep. No. UCB/EERC, 88, 17.

[2] AISC Committee. (2010). Specification for structural steel buildings (ANSI/AISC 360-10). American Institute of Steel Construction, Chicago-Illinois.

[3] Aki, K. (1993). Local site effects on weak and strong ground motion. Tectonophysics, 218(1-3), 93-111.

[4] Ali, U., & Ali, S. A. (2020). Comparative response of Kashmir Basin and its surroundings to the earthquake shaking based on various site effects. Soil Dynamics and Earthquake Engineering, 132, 106046.

[5] Ancheta, T. D., Darragh, R. B., Stewart, J. P., Seyhan, E., Silva, W. J., Chiou, B. S. J., ... & Donahue, J. L. (2014). NGA-West2 database. Earthquake Spectra, 30(3), 989-1005.

[6] Anderson, J. G., Bodin, P., Brune, J. N., Prince, J., Singh, S. K., Quaas, R., & Onate, M. (1986). Strong ground motion from the Michoacan, Mexico, earthquake. Science, 233(4768), 1043-1049.

[7] Bagchi, S., Sarkar, A., & Bagchi, A. (2021). Efficient Arrangement of Friction Damped Bracing System (FDBS) for Multi-storey Steel Frame. In Recent Advances in Computational Mechanics and Simulations (pp. 397-412). Springer, Singapore.

[8] Bakir, B. S., Sucuoglu, H., & Yilmaz, T. (2002). An overview of local site effects and the associated building damage in Adapazari during the 17 August 1999 Izmit earthquake. Bulletin of the Seismological Society of America, 92(1), 509-526.

[9] Behrou, R., Haghpanah, F., & Foroughi, H. (2017). Seismic site effect analysis for the city of Tehran using equivalent linear ground response analysis. International Journal of Geotechnical Engineering, 1-9.

[10] Behrou, R., Haghpanah, F., & Foroughi, H. (2018). Empirical seismic site effect analysis for the city of Tehran using H/V and methods. International Journal of Geotechnical Engineering, 1-9.

[11] Bergman, D. M., & Hanson, R. D. (1993). Viscoelastic mechanical damping devices tested at real earthquake displacements. Earthquake Spectra, 9(3), 389-417.

[12] Building and Housing Research Center (BHRC). (2014). Iranian Code of Practice for Seismic Resistant Design of Buildings (Standard No. 2800), 4rd Edition, Tehran, Iran.

[13] Cultrera, G., Mucciarelli, M., & Parolai, S. (2011). The L'Aquila earthquake—A view of site effects and building behavior from temporary networks.

[14] Filiatrault, A., & Cherry, S. (1986). Seismic tests of friction damped steel frames. Dynamic Response of Structures (pp. 138-145). ASCE.

[15] Filiatrault, A., & Cherry, S. (1990). Seismic design spectra for friction-damped structures. Journal of Structural Engineering, 116(5), 1334-1355.

[16] Kavand, A., & Yazdi, M. (2019). Kinematic interaction of pile groups with liquefied soil during lateral spreading based on 1g shake table tests. 7th International Conference on Earthquake Geotechnical Engineering, 3218–3225. Roma, Italy.

[17] Khansefid, A., & Ahmadizadeh, M. (2016). An investigation of the effects of structural nonlinearity on the seismic performance degradation of active and passive control systems used for supplemental energy dissipation. Journal of Vibration and Control, 22(16), 3544-3554.

[18] Lee, D., & Taylor, D. P. (2001). Viscous damper development and future trends. The Structural Design of Tall Buildings, 10(5), 311-320.

[19] Mazza, F., Vulcano, A., Mazza, M., & Mauro, G. (2013, January). Modeling and nonlinear seismic analysis of framed structures equipped with damped braces. In 7th WSEAS International Conference on Computer Engineering and Applications.

[20] Nabid, N., Hajirasouliha, I., Margarit, D. E., & Petkovski, M. (2020, October). Optimum energy based seismic design of friction dampers in RC structures. In Structures (Vol. 27, pp. 2550-2562). Elsevier.

[21] Navarro, M., García-Jerez, A., Alcalá, F. J., Vidal, F., Aranda, C., & Enomoto, T. (2012, September). Analysis of site effects, building response and damage distribution observed due to the 2011 Lorca, Spain, earthquake. In 15th World Conference of Earthquake Engineering 15WCEE (pp. 24-28).

[22] Newmark, N. M. (1959). A method of computation for structural dynamics. Journal of the engineering mechanics division, 85(3), 67-94.

[23] Pall, A. S. (1979). Limited slip bolted joints: a device to control the seismic response of large panel structures (Doctoral dissertation, Concordia University).

[24] Pall, A., & Pall, R. T. (2004, August). Performance-based design using pall friction dampers-an economical design solution. In 13th World Conference on Earthquake Engineering, Vancouver, BC, Canada (Vol. 71).

[25] Panah, A. K., & Nouri, A. (2016). An Investigation of Local Site Effects Using Linear and Nonlinear analysis and Comparison Between Them. Civil Engineering Journal, 2(4), 113-122.

[26] PEER Ground Motion Database. https://ngawest2.berkeley.edu/

[27] Ramirez, J. D. M., & Tirca, L. (2012, September). Numerical Simulation and Design of Friction-Damped Steel Frame Structures damped. In Proceedings of 15th World Conference in Earthquake Engineering, Lisbon, Portugal (pp. 24-28).

[28] Román-De La Sancha, A., Mayoral, J. M., Hutchinson, T. C., Candia, G., Montgomery, J., & Tepalcapa, S. (2019). Assessment of fragility models based on the Sept 19th, 2017 earthquake observed damage. Soil Dynamics and Earthquake Engineering, 125, 105707.

[29] Sadeghi, A., Abdollahzadeh, G., Rajabnejad, H., & Naseri, S. A. (2020). Numerical analysis method for evaluating response modification factor for steel structures equipped with friction dampers. Asian Journal of Civil Engineering, 1-18.

[30] Sanchez-Sesma, F. J. (1987). Site effects on strong ground motion. Soil Dynamics and Earthquake Engineering, 6(2), 124-132.

[31] Sanghai, S. S., & Pawade, P. Y. (2019). A Review on:'Performance of Friction Damper for Response Control of Buildings Considering Effect of Soil–Structure Interaction'. In Smart Technologies for Energy, Environment and Sustainable Development (pp. 335-346). Springer, Singapore.

[32] Sanghai, S., & Pawade, P. (2021). Optimal placement of friction dampers in building considering nonlinearity of soil. Innovative Infrastructure Solutions, 6(1), 1-18.

[33] Sepehri, A. (2016). Analyze and Design of Seismic Dampers and Base Isolators Accordance with ASCE7-10 by PERFORM3D-SAP2000 and OpenSEES. Elme Omran Publishing. (in Persian)

[34] Symans, M. D., Charney, F. A., Whittaker, A. S., Constantinou, M. C., Kircher, C. A., Johnson, M. W., & McNamara, R. J. (2008). Energy dissipation systems for seismic applications: current practice and recent developments. Journal of structural engineering, 134(1), 3-21.

[35] Taiyari, F., Mazzolani, F. M., & Bagheri, S. (2019). Damage-based optimal design of friction dampers in multistory chevron braced steel frames. Soil Dynamics and Earthquake Engineering, 119, 11-20.

[36] Tirca, L. (2015). Friction dampers for seismic protections of steel buildings subjected to earthquakes: Emphasis on structural design. Encyclopedia of Earthquake Engineering, Springer, Berlin, 1058, 1070.

[37] Trifunac, M. D. (2016). Site conditions and earthquake ground motion–A review. Soil dynamics and earthquake engineering, 90, 88-100.

[38] Vaseghi, J., Navaei, S., Navayinia, B., & Roshantabari, F. (2009). A parametric assessment of friction damper in eccentric braced frame. World Academy of Science, Engineering and Technology, 58, 208-212.

[39] Voica, T. F., & Stratan, A. (2020, March). Review of damage-tolerant solutions for improved seismic performance of buildings. In IOP Conference Series: Materials Science and Engineering (Vol. 789, No. 1, p. 012062). IOP Publishing.

[40] Wen, Z. P., Gao, M. T., Zhao, F. X., Li, X. J., Lu, H. S., & He, S. L. (2006). Seismic vulnerability estimation of the building considering seismic environment and local site condition. ACTA Seismologica Sinica, 19(3), 292-298.

[41] Whittaker, A. S., Bertero, V. V., Thompson, C. L., & Alonso, L. J. (1991). Seismic testing of steel plate energy dissipation devices. Earthquake Spectra, 7(4), 563-604.